Accepted refereed manuscript of:

Lopes-Marques M, Ozório R, Amaral R, Tocher DR, Monroig O & Costa Castro LF (2017) Molecular and functional characterization of a fads2 orthologue in the Amazonian teleost, Arapaima gigas, *Comparative Biochemistry and Physiology - Part B: Biochemistry and Molecular Biology*, 203, pp. 84-91.

DOI: 10.1016/j.cbpb.2016.09.007

Molecular and functional characterization of a *fads2* orthologue in the Amazonian teleost, *Arapaima gigas*

Mónica Lopes-Marques[1,2], Rodrigo Ozório[1,2], Ricardo Amaral[3], Douglas R. Tocher[4], Óscar Monroig[4*] and L. Filipe C. Castro[1,5*]

[1]CIIMAR – Interdisciplinary Centre of Marine and Environmental Research, U. Porto – University of Porto, Porto, Portugal

[2]ICBAS - Institute of Biomedical Sciences Abel Salazar, U. Porto - University of Porto, Portugal

[3]Universidade Federal do Acre, Brazil

[4]Institute of Aquaculture, Faculty of Natural Sciences, University of Stirling, Stirling FK9 4LA, Scotland, UK

[5]Department of Biology, Faculty of Sciences, U. Porto - University of Porto, Portugal

*Contributed equally to this work.

Correspondence to: filipe.castro@ciimar.up.pt; oscar.monroig@stir.ac.uk

Keywords: *Arapaima gigas*, Fatty acid desaturase (Fads), Long-chain polyunsaturated fatty acids (LC-PUFAs), teleosts, evolution

Abstract

The Brazilian teleost *Arapaima gigas* is an iconic species of the Amazon. In recent years a significant effort has been put into the farming of arapaima to mitigate overfishing threats. However, little is known regarding the nutritional requirements of *A. gigas* in particular those for essential fatty acids including the long-chain polyunsaturated fatty acids (LC-PUFA) eicosapentaenoic acid (EPA) and docosahexaenoic acid (DHA). The ability to biosynthesize LC-PUFA is dependent upon the gene repertoire of fatty acyl desaturases (Fads) and elongases (Elovl), as well as their fatty acid specificities. In the present study we characterized both molecularly and functionally an orthologue of the desaturase fatty acid desaturase 2 (*fads2*) from *A. gigas*. The isolated sequence displayed the typical desaturase features, a cytochrome b_5-domain with the heme-binding motif, two transmembrane domains and three histidine-rich regions. Functional characterization of *A. gigas fads2* showed that, similar to other teleosts, the *A. gigas fads2* exhibited a predominant Δ6 activity complemented with some capacity for Δ8 desaturation. Given that *A. gigas* belongs to one of the oldest teleostei lineages, the Osteoglossomorpha, these findings offer a significant insight into the evolution LC-PUFA biosynthesis in teleosts.

Introduction

Long-chain polyunsaturated fatty acids (LC-PUFA) play vital roles in numerous biological processes. They participate in structural functions as major components of biomembranes and are also involved in processes such as the inflammatory response, reproduction (Wall et al., 2010; Robinson and Mazurak, 2013), and neural development (Perica and Delaš, 2011) and can have beneficial effects in pathological conditions such as cardiovascular disease (Psota et al., 2006; Jump et al., 2012). LC-PUFA are often defined as compounds with 20 to 24 carbon atoms and three or more double bonds (unsaturations) and can be classified into two main groups: the omega-6 (ω6 or n-6) and the omega-3 (ω3 or n-3) LC-PUFA, based upon the position of the first double bond in relation to the methyl end carbon (CH_3) (Monroig et al., 2011a). LC-PUFA of the n-6 and n-3 series can be of dietary origin or, alternatively, they can be biosynthesized from dietary essential fatty acids (EFA) such as linoleic acid (LA, 18:2n-6) and α-linolenic acid (ALA, 18:3n-3), respectively, through a series of sequential biochemical reactions, mediated by elongation of very long-chain fatty acid protein (Elovl) and fatty acyl desaturases (Fads).

The ability to endogenously synthesize LC-PUFA from dietary fatty acids (FA) differs markedly among vertebrate species (Rivers et al., 1975; Bauer, 1997; Tocher, 2003; Burdge and Calder, 2005; Fonseca-Madrigal et al., 2014; Castro et al., 2016; Monroig et al., 2016a; Monroig et al., 2016b). This variation may be primarily attributed to differences in the *elovl* and *fads* gene repertoire, as well as their associated fatty acid substrate specificities. For instance, mammals have several *FADS* genes of which *FADS1* encodes a Δ5 desaturase and *FADS2* encodes a desaturase with Δ6 preference, in addition to Δ4 activity reported in some mammals (Park et al., 2009; Park et al., 2015) . In contrast, teleost fish examined to date have been found to possess exclusively *FADS2* orthologues (Castro et al., 2012; Castro et al., 2016). However, while mammalian FADS enzymes are essentially mono-functional, mechanisms of bifunctionalization (i.e., acquisition of additional/alternative substrate specificities) have been described in several teleost Fads2. Thus, Fads2 with dual Δ6Δ5

desaturase activities have been described in *Danio rerio* (Hastings et al., 2001), *Siganus canaliculatus* (Li et al., 2010), *Oreochromis niloticus* (Tanomman et al., 2013), *Chirostoma estor* (Fonseca-Madrigal et al., 2014) and *Clarias gariepinus* (Oboh et al., 2016). In addition, *S. canaliculatus* and *C. estor* possess a duplicated *Fads2* that exhibit Δ4 desaturase activity (Li et al., 2010; Fonseca-Madrigal et al., 2014), a type of enzyme also found in *Solea senegalensis* (Morais et al., 2012) and *Channa striata* (Kuah et al., 2015). Moreover, in agreement with the abilities reported in the baboon Δ6-desaturase (Park et al., 2009), the majority of teleost Fads2 desaturases have been demonstrated to possess the capability for Δ8 desaturation (Monroig et al., 2011b). Overall the complement of LC-PUFA biosynthetic enzymes, namely FADS and ELOVL, as well as their functionalities, dictates the ability of a species for the conversion of C_{18} PUFA (LA and ALA) into physiologically important LC-PUFA including arachidonic acid (ARA, 20:4n-6), eicosapentaenoic acid (EPA, 20:5n-3) and docosahexaenoic acid (DHA, 22:6n-3) (Bell and Tocher, 2009; Castro et al., 2016). Importantly, the investigation of Fads and Elovl in fish has primarily focused on farmed species since both Fads and Elovl capabilities underpin the efficiency of these fish species to utilize the C_{18} PUFA present in vegetable oils (VO) currently used as sustainable replacements for dietary fish oils (FO) in aquafeeds (Tocher, 2010). Therefore a clear understanding of LC-PUFA biosynthesis pathways is critical to understand the potential limitations of farmed fish species and for the implementation of dietary strategies to fulfil essential requirements and ensure normal growth and development in captivity.

An iconic species of the Amazon, so-called “pirarucú” (*Arapaima gigas*), is one of the largest freshwater and air-breathing fishes in the world, and has been extensively fished since the 18th century (Veríssimo, 1895; Goulding, 1980). In the early 1970’s over-exploitation of *A. gigas* led to its near extinction (Goulding, 1980) and listing in CITES (Convention on International Trade in Endangered Species of Wild Fauna and Flora). To overcome this threat, considerable effort has been put into developing the sustainable farming of this species. However, despite some important advances, critical knowledge in key areas such as

94 physiology and nutrition is still scarce in this species. Much of the published research on *A.*
95 *gigas* has focused on the understanding and evolution of the air-breathing capacity (Brauner
96 et al., 2004; Gonzalez et al., 2010), general health and aquaculture practices (Ribeiro et al.,
97 2011; Bezerra et al., 2014) and, more recently, the potential use of *A. gigas* scales as
98 biomaterials (Torres et al., 2015). In contrast, few studies have addressed the dietary
99 requirements of *A. gigas* (Ituassú et al., 2005; Andrade et al., 2007; Ribeiro et al., 2011),
100 stressing the need for a broader understanding of the metabolism of this carnivorous species.
101 Here, we describe the isolation and functional characterization of a cDNA from *A. gigas*
102 orthologous to *fads2* desaturases, key enzymes in LC-PUFA biosynthetic pathways and
103 crucial elements in determining EFA requirements in this species. The phylogenetic position
104 of *A. gigas* within one of the most ancient teleost lineages, the Osteoglossomorpha, brings
105 new insights into the evolution of the LC-PUFA biosynthesis cascade in both fish and
106 vertebrates in general.

107

108 **Materials and Methods**

109 ***Molecular cloning of the A. gigas fads gene***

110 Total RNA was extracted from a range of *A. gigas* tissues using the Illustra RNAspin Mini kit
111 (GE Healthcare, UK). The RNA extraction process included an on-column DNase I treatment
112 (provided in the kit). RNA integrity was assessed on a 1 % agarose TAE gel stained with
113 GelRed™ nucleic acid stain (Biotium, Hayward, CA, USA). The Quant-iT™ RiboGreen®
114 RNA Assay Kit (Life Technologies, Carlsbad, CA, USA) was used to measure total RNA
115 concentration. Reverse transcription reactions were performed with the iScript cDNA
116 Synthesis Kit (Bio-Rad, Hercules, CA, USA).

117 *Arapaima gigas* FADS gene was isolated in three main steps. First, degenerate primers
118 targeting the Fads gene were designed using CODEHOP (Rose et al., 2003) available at
119 http://blocks.fhcrc.org/codehop.html. The initial polymerase chain reaction (PCR) was

performed with a degenerate primer set and Flash High-Fidelity PCR Master Mix (Thermo Fisher Scientific, Waltham, USA), set for a final volume of 20 µl, with 500 nM of sense and antisense primers, and 1 µl of *A. gigas* cDNA pool (see Table 1 for primers, PCR conditions). In the second step, the partial *fads* sequence was further extended by Rapid amplification of cDNA ends (RACE) PCR using as template 5' and 3' RACE ready cDNA prepared with SMARTer™ RACE cDNA Amplification Kit (Clontech, CA, USA). Gene specific primers for RACE were designed using the previously isolated fragment and RACE PCR was performed with Flash High-Fidelity PCR Master Mix (Thermo Fisher Scientific) using 1 µl of gene specific primer combined with 2 µl Universal primer mix (Clontech) (see table 1 for primers and PCR conditions). The resulting 5´and 3´sequences were assembled to produce the full open reading frame (ORF) *fads*-like cDNA. In the final step, the full ORF of *A. gigas* FADS was isolated using 1 µl of *A. gigas* cDNA pool, and Flash High-Fidelity PCR Master Mix (Thermo Fisher Scientific, Waltham, USA), set for a final volume of 20 µl, with 500 nM of sense and antisense primers (see table 1 for primers and PCR conditions). In each step resulting PCR products were analysed in 1 % agarose gel, purified with NZYGelpure (NZYTech, Lisbon, Portugal) and confirmed by sequencing (GATC Biotech Constance, Germany). The final, full ORF sequence was translated and submitted to pFAM and NCBI for blastp searches retrieving Fads-like profile (Accession number: KX809739).

Sequence collection, phylogenetic and 2D structural analysis

Fads amino acid (aa) sequences were retrieved from Genbank and Ensembl (for accession numbers see Table 2). Sequences were aligned with MAFFT using the L-INS-i method (Katoh and Toh, 2008). The sequence alignment was stripped from all columns containing gaps leaving 374 gap-free sites for phylogenetic analysis. Maximum likelihood phylogenetic analysis was performed in PhyML v3.0 server (Guindon et al., 2010) using smart model selection resulting in LG +G+I+F, and branch support was calculated using 1000 bootstraps.

146 Using the same alignment a second Bayesian phylogenetic analysis was performed using
147 MrBayes v3.2.3 available in CIPRES Science Gateway V3.3 (Miller et al., 2015). MrBayes
148 was run for 1 million generations with the following parameters: rate matrix for aa=mixed,
149 nruns=2, nchains=4, temp=0.2, sampling set to 500 and burin to 0.25. The resulting trees
150 were visualized in Fig Tree V1.3.1 available at http://tree.bio.ed.ac.uk/software/figtree/ and
151 rooted at mid-point. *A. gigas* aa sequence was submitted to TOPCONS web server for
152 prediction of 2D topology, with all parameters set to default (http://topcons.net/) (Tsirigos et
153 al., 2015), and results visualized using Potter web application (http://wlab.ethz.ch/protter)
154 (Omasits et al., 2014).

155 ***Yeast expression assays and fatty acid analysis***

156 The *A. gigas fads* ORF was isolated with two sequential PCR with Flash High-Fidelity
157 PCR Master Mix (Thermo Fisher Scientific, USA) as described above. The first PCR was
158 performed with an *A. gigas* cDNA pool and primers (AgigasFADS_ORF_F and
159 AgigasFADS_ORF_R, Table 1) targeting the full ORF. The PCR product was diluted (1:50)
160 and used as template for the second PCR performed with primers containing restriction sites
161 for *Kpn*I (AgigasFADS_pYES_KpnI_F) and *Xba*I (AgigasFADS_pYES_XbaI_R) (Table 1).
162 The final PCR product was purified and digested with the appropriate restriction enzymes and
163 cloned into the yeast expression vector pYES2 (Invitrogen, CA, USA). Transformation and
164 culture of yeast *Saccharomyces cerevisiae* were conducted as previously described (Hastings
165 et al., 2001; Agaba et al., 2004; Oboh et al., 2016). Briefly, transgenic yeast expressing the *A.*
166 *gigas fads* ORF were grown in the presence of PUFA including Δ6 (18:3n-3 and 18:2n-6), Δ8
167 (20:2n-6 and 20:3n-3), Δ5 (20:4n-3; 20:3n-6) and Δ4 (22:5n-3 and 22:4n-6) desaturase
168 substrates. PUFA substrates, added as sodium salts, were supplemented in the yeast medium
169 at final concentrations of 0.5 mM (C_{18}), 0.75 mM (C_{20}) and 1.0 mM (C_{22}) as uptake efficiency
170 decreases with increasing chain length (Zheng et al., 2009). After 48 h of incubation, yeast
171 were harvested, washed and total lipid extracted by homogenization in chloroform/methanol
172 (2:1, v/v) containing 0.01 % BHT (Monroig et al., 2013). Fatty acyl methyl esters (FAME)

were prepared from total lipids extracted from harvested cells and identified based on GC retention times and confirmed by GC-MS as described previously (Hastings et al., 2001; Li et al., 2010). FA desaturation efficiencies from exogenously added PUFA substrates were calculated by the proportion of substrate FA converted to a desaturated product as (product area/(product area + substrate area)) x 100.

Results

Sequence conservation and topology prediction

The isolated *A. gigas* sequence was translated and submitted to BLASTp and to PFam to validate the *fads*-like profile and identify the main protein domains. BLASTp searches showed that the *A. gigas* sequence had highest identity scores with *fads2* desaturases from other teleost species (results not shown), while the PFam search identified two main domains typical of Fads enzymes: a cytochrome b_5-like heme/steroid binding domain (15 - 88 aa) and FA desaturase domain (150 - 412 aa). To further characterize, the *A. gigas* Fads-like protein was aligned with four known and fully characterized Fads aa sequences from *D. rerio* (NCBI Protein accession no **Q9DEX7.1**), *Salmo salar* (NCBI Protein accession no **NP_001117047.1**), *O. niloticus* (NCBI Protein accession no **AGV52807.1**) and *Homo sapiens* (NCBI Protein accession no **NP_004256.1**) (Fig. 1A). The *A. gigas* sequence showed highest degree of pairwise identity with the *S. salar* Fads2 (86.1 %), followed by Fads2 from *O. niloticus* (83.9 %), *D. rerio* (82.8 %) and *H. sapiens* (79.3 %), revealing a high degree of cross-species conservation. Additionally, using *H. sapiens* FADS2 sequence as a reference, several sequence signature motifs of Fads enzymes were identified: the heme binding motif HPGG and three histidine boxes HXXXH, HXXHH and QXXHH, which are presumed to form the Fe-binding active center of the enzyme (Los and Murata, 1998; Pereira et al., 2003) (Fig. 1A). The heme binding motif was totally conserved in Fads from all species analyzed including *A. gigas.* In the first histidine box two distinct patterns were observed: HD**Y**GH in *H. sapiens* and *S. salar*, while *A. gigas*, *D. rerio* and *O. niloticus* showed the signature

200 HD**F**GH with the replacement of a tyrosine (Y) by a phenylalanine (F) (Fig. 1A). In the
201 second histidine box, all analyzed species presented HF**Q**HH with the exception of *O.*
202 *niloticus*, whose Fads2 presents HF**R**HH (Fig. 1A). Full conservation of the third histidine
203 box was found across all the analyzed species.

204 Regarding the 2D topology prediction, all calculation methods were consistent in
205 predicting that *A. gigas* Fads-like displayed four membrane spanning domains, and that the N-
206 and the C-terminals, as well as the three histidine motifs, were oriented towards the cytosol
207 (Supplementary Material 1). Interestingly, the residues involved in regioselectivity were
208 localized at the base of the third membrane spanning domain (Fig. 1B). The topology
209 predicted for the *A. gigas* Fads2 was thus consistent with the structural organization proposed
210 in previous reports for other Fads-like desaturases (Los and Murata, 1998; Meesapyodsuk et
211 al., 2007; Lim et al., 2014).

212 ***Phylogenetic analysis of Fads-like ORF from A. gigas***

213 Two phylogenetic analyses were conducted using the same data set consisting of aa
214 sequence alignment between the newly cloned *A. gigas* putative Fads with FADS1 and
215 FADS2 desaturase sequences from eighteen vertebrate species (mammals - *H. sapiens, M.*
216 *domestica* birds – *G. gallus*, reptiles - *A. sinensis,* coelacanth - *L. chalumnae,* teleosts - *G.*
217 *morhua*, *T. maccoyii*, *O. niloticus*, *S. salar*, and *D. rerio*, chondrichthyans - *S. canicula*, *C.*
218 *milii* and one invertebrate (*B. floridae*). In both cases the tree topology showed two well-
219 supported clades, one corresponding to the FADS1 and the second corresponding to the
220 FADS2, being both trees out grouped by invertebrate FADS from *B. floridae*. The *A. gigas*
221 Fads-like sequence strongly grouped (930 bootstraps or 1 posterior probabilities) within the
222 teleost group composed of all Fads2 sequences. Out grouping the teleost clade we find
223 tetrapod and chondrichthyans Fads2 desaturases, indicating that the *A. gigas* putative Fads is
224 a true *fads2* orthologue. However, desaturases with different substrate preferences, for
225 example *D. rerio* and *O. niloticus* Fads2 that are bifunctional Δ6Δ5 desaturases (Hastings et

al., 2001; Tanomman et al., 2013), and *G. morhua* and *S. salar* Fads2 that have been reported as unifunctional Δ6 desaturases (Zheng et al., 2005; Monroig et al., 2010) were found within the teleost clade.

Functional analysis of Fads2 in A. gigas

Functional characterization of the *A. gigas* desaturase was performed with using a well-established heterologous system consisting of yeast *S. cerevisiae* expressing the ORF of the *A. gigas fads2* and grown in the presence of potential desaturase PUFA substrates (Hastings et al., 2001; Agaba et al., 2004; Fonseca-Madrigal et al., 2014). FA profile of yeast transformed with the empty pYES2 plasmid (control) consisted of the yeast endogenous FA including 16:0, 16:1 isomers (16:1n-9 and 16:1n-7), 18:0, and 18:1 isomers (18:1n-9 and 18:1 n-7) and whichever exogenously PUFA substrate was added (data not shown). These results confirmed that the yeast endogenous enzymes were not active on the exogenously added PUFA substrates (Agaba et al., 2005). On the other hand, yeast transformed with the ORF of the *A. gigas fads2* showed additional peaks when grown in the presence of 18:3n-3, 18:2n-6, 20:3n-3 and 20:2n-6 (Fig. 3). Thus, transgenic yeast expressing the *fads2* had the ability to desaturate 18:3n-3 and 18:2n-6 to 18:4n-3 (Fig. 3A) and 18:3n-6 (Fig. 3B), respectively, showing this enzyme has Δ6 desaturase activity. Moreover, transgenic yeast supplemented with 20:3n-3 and 20:2n-6 produced additional peaks identified as 20:4n-3 (Fig. 3C) and 20:3n-6 (Fig. 3D), respectively, showing that the *A. gigas fads2* had also Δ8 desaturase activity. Therefore, the data confirmed that the cloned *A. gigas fads2* encoded an enzyme with Δ6 and Δ8 desaturase specificities. Conversions obtained in the yeast expression system suggested that the *A. gigas* Fads2 has Δ6 as the most prominent activity and a preference for n-3 fatty acid substrates compared with n-6 substrates for each homologous FA substrate pair (Δ6 or Δ8) considered (Table 3). Neither Δ5 nor Δ4 activities were detected in yeast (Fig. 3E-H).

252 **Discussion**

253 Fads are, together with Elovl, key enzymes in LC-PUFA biosynthetic pathways (Castro et al.,
254 2016; Monroig et al., 2016b)). The sequential and concerted action of both enzymes defines
255 the ability of a given species to endogenously synthesize physiologically relevant LC-PUFA
256 including ARA, EPA or DHA (Bell and Tocher, 2009). The investigation of the molecular
257 components of LC-PUFA biosynthetic pathway in fish has been an active field of research
258 over the last decade (Agaba et al., 2005; Zheng et al., 2009; Monroig et al., 2011b; Castro et
259 al., 2012; Monroig et al., 2012; Carmona-Antonanzas et al., 2013; Castro et al., 2016). This is
260 particularly true in farmed fish species where a full understanding of LC-PUFA biosynthesis
261 capacities is crucial to successfully grow fish on diets that are necessarily being formulated
262 with ever-increasing levels of VO (rich in C_{18} PUFA but devoid of LC-PUFA) as primary
263 lipid sources to replace FO (Turchini et al., 2009). Overall, these studies have highlighted a
264 surprisingly diverse and interesting pattern among Fads substrate specificities (Fonseca-
265 Madrigal et al., 2014).

266 The primary objective of the present study was the molecular cloning and functional
267 characterization of a desaturase of the Amazonian teleost *A. gigas*. This freshwater species
268 with aquaculture potential (Cavero et al., 2003) has been barely investigated in terms of
269 nutritional requirements. In addition, *A. gigas* belongs to the Osteoglossiformes, a teleost
270 order that has been considered to be the most basal of living teleosts (Nelson, 1994), therefore
271 bringing a fresh perspective on the functional diversification of the desaturases in teleosts.
272 The isolated Fads2 sequence of *A. gigas* showed all the typical features of fatty acyl (also
273 known as "front-end") desaturases when subjected to BLASTp and to PFam searches.
274 Furthermore, detailed sequence alignment analysis revealed that the unique structure of Fads-
275 like enzymes was preserved in *A. gigas* Fads2 that contained three highly conserved histidine
276 boxes, as well as the heme motif within the cytochrome b_5-like domain, which are considered
277 to be involved in the formation of the desaturase catalytic centre (Shanklin et al., 1994; Los
278 and Murata, 1998; Tocher et al., 1998). The 2D topology analysis of *A. gigas* Fads2 predicted

four transmembrane domains TM1: 124-145, TM2: 151-172, TM3: 258-279, TM4: 300-321, that oriented the three histidine boxes and the cytochrome b_5-like domain to the cytosol, consistent with the structural organization proposed in previous reports (Los and Murata, 1998; Meesapyodsuk et al., 2007; Lim et al., 2014). Among the three histidine boxes, two distinct patterns were observed in the first histidine box in the Fads2, with *A. gigas*, *D. rerio* and *O. niloticus* having the signature HDFGH, whereas a replacement of a phenylalanine (F) by tyrosine (Y) occurs for *H. sapiens* and *S. salar* Fads2. This replacement was predicted to not affect the mandatory/canonical histidine residues within each box. Additionally the abovementioned aa substitution was not expected to have any major functional impact, possibly due to the fact that these two aa residues share very similar biochemical properties (Betts and Russell, 2003). In contrast, differences were found within the residues previously proposed to participate in the regioselectivity of these enzymes (Hsa:279Phe - 282Gln; Dre:279Phe - 282Gln, Oni: 280Phe - His283, Ssa: 289Phe-292Gln; Agi: 273Phe - 276Gln) (Meesapyodsuk et al., 2007; Lim et al., 2014), possibly accounting for the different Fads activities observed in these species.

All *fads* characterized so far from teleosts are orthologous to *FADS2*, which performs primarily Δ6 desaturations in mammals (Guillou et al., 2010). This is further supported by the herein phylogenetic analysis of *A. gigas fads*, together with phylogenetic analyses reported previously (Zheng et al., 2004; Monroig et al., 2011b; Liu et al., 2014). However, the teleost Fads exhibit a wide range of PUFA specificities (Hastings et al., 2001; Hastings et al., 2004; Li et al., 2010; Monroig et al., 2012; Xie et al., 2014), underscoring a "*functional plasticity"* that has been previously attributed as a consequence of adaptation to availability of LC-PUFA in variable habitats and trophic levels (Tocher, 2010; Monroig et al., 2011b; Castro et al., 2012; Monroig et al., 2012; Fonseca-Madrigal et al., 2014). Thus, Fads2 with dual Δ6Δ5 activity have been cloned from *D. rerio* (Hastings et al., 2001), *S. canaliculatus* (Li et al., 2010), *O. niloticus* (Tanomman et al., 2013), *C. estor* (Fonseca-Madrigal et al., 2014), and *C. gariepinus* (Oboh et al., 2016). Moreover, teloest Fads2 with Δ4 desaturase activity have been

306 found in *S. canaliculatus* (Li et al., 2010), *S. senegalensis* (Morais et al., 2012) and *C. striata*
307 (Kuah et al., 2015). Interestingly, the human *FADS2* gene product has been recently
308 demonstrated to have the ability for direct Δ4 desaturation of 22:5n-3 to 22:6n-3 (Park et al.,
309 2015). Nevertheless, the majority of functionally characterized teleost Fads2 are essentially
310 Δ6 desaturase enzymes as reported in a variety of teleost fish species including gilthead
311 seabream, rainbow trout, Atlantic salmon (three genes), turbot, cobia, European seabass,
312 barramundi, black seabream, nibe croaker, Northern bluefin tuna, meagre, Japanese eel and
313 orange spotted grouper (Castro et al., 2016). In agreement, the *A. gigas* Fads2 was
314 demonstrated to be a Δ6 desaturase able to convert 18:3n-3 and 18:2n-6 to 18:4n-3 and 18:3n-
315 6, respectively.

316 However, in addition, the *A. gigas* Fads2 showed capability for Δ8 desaturation, since it
317 was capable of converting both 20:3n-3 and 20:2n-6 into 20:4n-3 and 20:3n-6, respectively.
318 This activity was first reported in the baboon FADS2 (Park et al., 2009) and subsequently
319 described in a range of fish Fads2 enzymes (Monroig et al., 2011b). The capability for Δ8
320 desaturation appears widespread in Fads2 characterized from fish (Monroig et al., 2011b;
321 Monroig et al., 2013; Wang et al., 2014; Kabeya et al., 2015; Oboh et al., 2016), with few
322 exceptions represented by the Atlantic salmon and rainbow trout Δ5 Fads2, as well as the
323 striped snakehead Δ4 Fads2 (Monroig et al., 2011b; Kuah et al., 2015; Abdul Hamid et al.,
324 2016). Interestingly, it appeared that, generally, Fads2 from marine teleosts had relatively
325 high Δ8 desaturase ability compared to their freshwater and salmonid counterparts (Monroig
326 et al., 2011b). Consequently, the Δ6:Δ8 desaturation ratio varies among teleost Fads2, with
327 marine species having relatively low Δ6:Δ8 ratios, while freshwater and salmonid species
328 having higher Δ6:Δ8 ratios. The *A. gigas* Fads2 had a Δ6:Δ8 ratio of 4.4 for n-3 PUFA
329 substrates (25.8 : 5.8), and thus more within the range of marine teleosts such as turbot (4.2)
330 or gilthead seabream (2.7) and far from freshwater species like rainbow trout (91.5) and
331 zebrafish (22.4). While it is unclear what the evolutionary drivers are for the high capacity for
332 Δ8 desaturation in *A. gigas* Fads2, having a Fads2 with the ability to operate as a Δ6

desaturase on ALA and LA, and as a Δ8 on 20:3n-3 and 20:2n-6, may confer an advantage to this species enabling production of 20:4n-3 and 20:3n-6, respectively, through two different pathways. Both 20:4n-3 and 20:3n-6 are substrates of Δ5 desaturase, an enzyme that, despite being absent in the vast majority of teleosts, is likely to be retained in basal teleosts such as Osteoglossidae, the family to which *A. gigas* belongs. In fact, a close relative to *A. gigas*, the Asian arowana (*Scleropages formosus*) also a basal teleost belonging to the Osteoglossidae, presents two predicted Fads-like sequences recently deposited in GenBank KPP61181.1 and KPP71333.1 (not included in phylogenetic analysis due to their partial nature) annotated as FADS2-like and delta 6 desaturase-like respectively. However, no functional characterization these genes is yet available. Further studies are required to fully confirm the presence or absence of Fads1 in basal teleost lineages.

In conclusion, we herein demonstrate that *A. gigas* possess a *fads2* gene with all the typical features of front-end desaturases. Moreover, the functional assays of the *A. gigas* Fads2 in yeast confirmed that, like the majority of teleost Fads2, the *A. gigas* orthologue exhibited Δ6 and Δ8 desaturase activities. Along with the Fads2 from the Japanese eel (Wang et al., 2014), the herein reported *A. gigas* represents the most ancient representative of the Fads gene family being investigated within the teleost clade.

Acknowledgements

This work was funded by the Projeto CAPES/Pró-Amazônia/Projeto Arapaima-Pirarucu/Universidade do Porto -CIIMAR. Fundação para a Ciência e a Tecnologia (FCT) PhD grant [grant number SFRH/BD/84238/2012] awarded to M.L-.M. The access to the Institute of Aquaculture laboratories was funded by the European Union‘s Seventh Framework Programme (FP7/2007-2013) [grant number 262336] (AQUAEXCEL), Transnational Access [Project Number 0095/06/03/13].

References

Abdul Hamid, N.K., Carmona-Antoñanzas, G., Monroig, Ó., Tocher, D.R., Turchini, G.M., Donald, J.A. 2016. Isolation and Functional Characterisation of a fads2 in Rainbow Trout (Oncorhynchus mykiss) with Δ5 Desaturase Activity. PLoS ONE 11(3): e0150770.

Agaba, M., Tocher, D.R., Dickson, C.A., Dick, J.R., Teale, A.J., 2004. Zebrafish cDNA encoding multifunctional Fatty Acid elongase involved in production of eicosapentaenoic (20:5n-3) and docosahexaenoic (22:6n-3) acids. Mar Biotechnol (NY) 6, 251-261.

Agaba, M.K., Tocher, D.R., Zheng, X., Dickson, C.A., Dick, J.R., Teale, A.J., 2005. Cloning and functional characterisation of polyunsaturated fatty acid elongases of marine and freshwater teleost fish. Comp. Biochem. Physiol. B. Biochem. Mol. Biol. 142, 342-352.

Andrade, J.I.A.d., Ono, E.A., de Menezes, G.C., Brasil, E.M., Roubach, R., Urbinati, E.C., Tavares-Dias, M., Marcon, J.L., Affonso, E.G., 2007. Influence of diets supplemented with vitamins C and E on pirarucu (*Arapaima gigas*) blood parameters. Comparative Biochemistry and Physiology Part A: Molecular & Integrative Physiology 146, 576-580.

Bauer, J.E., 1997. Fatty acid metabolism in domestic cats (*Felis catus*) and cheetahs (*Acinonyx jubatas*). Proc. Nutr. Soc. 56, 1013-1024.

Bell, M.V., Tocher, D.R., 2009. Biosynthesis of polyunsaturated fatty acids in aquatic ecosystems: general pathways and new directions, in: Martin Kainz, Michael T. Brett, Michael T. Arts (Eds.), Lipids in Aquatic Ecosystems. Springer New York, pp211-236.

Betts, M.J., Russell, R.B., 2003. Amino Acid Properties and Consequences of Substitutions, Bioinformatics for Geneticists. John Wiley & Sons, Ltd, 289-316.

Bezerra, R.F., Soares, M.d.C.F., Santos, A.J.G., Maciel Carvalho, E.V.M., Coelho, L.C.B.B., 2014. Seasonality Influence on Biochemical and Hematological Indicators of Stress and Growth of Pirarucu (*Arapaima gigas*), an Amazonian Air-Breathing Fish. The Scientific World Journal 2014, 6.

Brauner, C.J., Matey, V., Wilson, J.M., Bernier, N.J., Val, A.L., 2004. Transition in organ function during the evolution of air-breathing; insights from *Arapaima gigas*, an obligate air-breathing teleost from the Amazon. J. Exp. Biol. 207, 1433-1438.

Burdge, G.C., Calder, P.C., 2005. Conversion of alpha-linolenic acid to longer-chain polyunsaturated fatty acids in human adults. Reprod. Nutr. Dev. 45, 581-597.

Carmona-Antonanzas, G., Tocher, D.R., Taggart, J.B., Leaver, M.J., 2013. An evolutionary perspective on Elovl5 fatty acid elongase: comparison of Northern pike and duplicated paralogs from Atlantic salmon. BMC Evol Biol 13, 85.

391 Castro, L.F.C., Monroig, Ó., Leaver, M.J., Wilson, J., Cunha, I., Tocher, D.R., 2012. Functional
392 Desaturase Fads1 (Δ5) and Fads2 (Δ6) Orthologues Evolved before the Origin of Jawed Vertebrates.
393 PLoS ONE 7, e31950.

394 Castro, L.F.C., Tocher, D.R., Monroig, O., 2016. Long-chain polyunsaturated fatty acid biosynthesis in
395 chordates: Insights into the evolution of Fads and Elovl gene repertoire. Prog. Lipid Res. 62, 25-40.

396 Cavero, B.A.S., Ituassú, D.R., Pereira-Filho, M., Roubach, R., Bordinhon, A.M., Fonseca, F.A.L., Ono,
397 E.A., 2003. Uso de alimento vivo como dieta inicial no treinamento alimentar de juvenis de pirarucu.
398 Pesquisa Agropecuária Brasileira 38, 1011-1015.

399 Fonseca-Madrigal, J., Navarro, J.C., Hontoria, F., Tocher, D.R., Martínez-Palacios, C.A., Monroig, Ó.,
400 2014. Diversification of substrate specificities in teleostei Fads2: characterization of Δ4 and Δ6Δ5
401 desaturases of *Chirostoma estor*. J. Lipid Res. 55, 1408-1419.

402 Gonzalez, R.J., Brauner, C.J., Wang, Y.X., Richards, J.G., Patrick, M.L., Xi, W., Matey, V., Val, A.L.,
403 2010. Impact of Ontogenetic Changes in Branchial Morphology on Gill Function in *Arapaima gigas*.
404 Physiol. Biochem. Zool. 83, 322-332.

405 Goulding, M., 1980. Fishes and the Forest: Explorations in Amazonian Natural History. University of
406 California Press.

407 Guillou, H., Zadravec, D., Martin, P.G., Jacobsson, A., 2010. The key roles of elongases and
408 desaturases in mammalian fatty acid metabolism: Insights from transgenic mice. Prog. Lipid Res. 49,
409 186-199.

410 Guindon, S., Dufayard, J.F., Lefort, V., Anisimova, M., Hordijk, W., Gascuel, O., 2010. New
411 algorithms and methods to estimate maximum-likelihood phylogenies: assessing the performance of
412 PhyML 3.0. Syst Biol 59, 307-321.

413 Hastings, N., Agaba, M., Tocher, D.R., Leaver, M.J., Dick, J.R., Sargent, J.R., Teale, A.J., 2001. A
414 vertebrate fatty acid desaturase with Δ5 and Δ6 activities. Proc Natl Acad Sci USA 98, 14304-14309.

415 Hastings, N., Agaba, M., Tocher, D., Zheng, X., Dickson, C., Dick, J., Teale, A., 2004. Molecular
416 Cloning and Functional Characterization of Fatty Acyl Desaturase and Elongase cDNAs Involved in
417 the Production of Eicosapentaenoic and Docosahexaenoic Acids from α-Linolenic Acid in Atlantic
418 Salmon (*Salmo salar*). Mar. Biotechnol. 6, 463-474.

419 Ituassú, D.R., Pereira Filho, M., Roubach, R., Crescêncio, R., Cavero, B.A.S., Gandra, A.L., 2005.
420 Níveis de proteína bruta para juvenis de pirarucu. Pesquisa Agropecuária Brasileira 40, 255-259.

421 Jump, D.B., Depner, C.M., Tripathy, S., 2012. Omega-3 fatty acid supplementation and cardiovascular
422 disease: Thematic Review Series: New Lipid and Lipoprotein Targets for the Treatment of
423 Cardiometabolic Diseases. J. Lipid Res. 53, 2525-2545.

Kabeya, N., Yamamoto, Y., Cummins, S.F., Elizur, A., Yazawa, R., Takeuchi, Y., Haga, Y., Satoh, S., Yoshizaki, G., 2015. Polyunsaturated fatty acid metabolism in a marine teleost, Nibe croaker Nibea mitsukurii: Functional characterization of Fads2 desaturase and Elovl5 and Elovl4 elongases. Comp. Biochem. Physiol. Biochem. Mol. Biol. 188, 37-45.

Katoh, K., Toh, H., 2008. Recent developments in the MAFFT multiple sequence alignment program. Briefings in bioinformatics 9, 286-298.

Kuah, M.K., Jaya-Ram, A., Shu-Chien, A.C., 2015. The capacity for long-chain polyunsaturated fatty acid synthesis in a carnivorous vertebrate: Functional characterisation and nutritional regulation of a Fads2 fatty acyl desaturase with Delta4 activity and an Elovl5 elongase in striped snakehead (*Channa striata*). Biochim. Biophys. Acta 1851, 248-260.

Li, Y., Monroig, O., Zhang, L., Wang, S., Zheng, X., Dick, J.R., You, C., Tocher, D.R., 2010. Vertebrate fatty acyl desaturase with Δ4 activity. Proceedings of the National Academy of Sciences 107, 16840-16845.

Lim, Z., Senger, T., Vrinten, P., 2014. Four Amino Acid Residues Influence the Substrate Chain-Length and Regioselectivity of Siganus canaliculatus Δ4 and Δ5/6 Desaturases. Lipids 49, 357-367.

Liu, H., Guo, Z., Zheng, H., Wang, S., Wang, Y., Liu, W., Zhang, G., 2014. Functional characterization of a Δ5-like fatty acyl desaturase and its expression during early embryogenesis in the noble scallop *Chlamys nobilis* Reeve. Mol. Biol. Rep. 41, 7437-7445.

Los, D.A., Murata, N., 1998. Structure and expression of fatty acid desaturases. Biochimica et Biophysica Acta (BBA) - Lipids and Lipid Metabolism 1394, 3-15.

Meesapyodsuk, D., Reed, D.W., Covello, P.S., Qiu, X., 2007. Primary Structure, Regioselectivity, and Evolution of the Membrane-bound Fatty Acid Desaturases of *Claviceps purpurea*. J. Biol. Chem. 282, 20191-20199.

Miller, M.A., Schwartz, T., Pickett, B.E., He, S., Klem, E.B., Scheuermann, R.H., Passarotti, M., Kaufman, S., O'Leary, M.A., 2015. A RESTful API for Access to Phylogenetic Tools via the CIPRES Science Gateway. Evol Bioinform Online 11, 43-48.

Monroig, Ó., Zheng, X., Morais, S., Leaver, M.J., Taggart, J.B., Tocher, D.R., 2010. Multiple genes for functional 6 fatty acyl desaturases (Fad) in Atlantic salmon (*Salmo salar* L.): gene and cDNA characterization, functional expression, tissue distribution and nutritional regulation. Biochim. Biophys. Acta 1801, 1072-1081.

Monroig, Ó., Tocher, D.R., Navarro, J.C., 2011a. Long-chain polyunsaturated fatty acids in fish: recent advances on desaturases and elongases involved in their biosynthesis, in: L. Cruz-Suarez, D. Ricque-Marie, M. Tapia-Salazar, M. Nieto-López, D. Villarreal-Cavazos, J. Gamboa-Delgado, L. Hernández-

Hernández (Eds.), Décimo Primer Simposio Internacional de Nutrición Acuícola, San Nicolás de los Garza, N. L., México.

Monroig, Ó., Li, Y., Tocher, D.R., 2011b. Delta-8 desaturation activity varies among fatty acyl desaturases of teleost fish: high activity in delta-6 desaturases of marine species. Comp. Biochem. Physiol. B. Biochem. Mol. Biol. 159, 206-213.

Monroig, Ó., Wang, S., Zhang, L., You, C., Tocher, D.R., Li, Y., 2012. Elongation of long-chain fatty acids in rabbitfish *Siganus canaliculatus*: Cloning, functional characterisation and tissue distribution of Elovl5- and Elovl4-like elongases. Aquaculture 350–353, 63-70.

Monroig, Ó., Tocher, D.R., Hontoria, F., Navarro, J.C., 2013. Functional characterisation of a Fads2 fatty acyl desaturase with Δ6/Δ8 activity and an Elovl5 with C16, C18 and C20 elongase activity in the anadromous teleost meagre (*Argyrosomus regius*). Aquaculture 412–413, 14-22.

Monroig, Ó., Hontoria, F., Varó, I., Tocher, D.R., Navarro, J.C., 2016a. Investigating the essential fatty acids in the common cuttlefish *Sepia officinalis* (Mollusca, Cephalopoda): Molecular cloning and functional characterisation of fatty acyl desaturase and elongase. Aquaculture 450, 38-47.

Monroig, Ó., Lopes-Marques, M., Navarro, J.C., Hontoria, F., Ruivo, R., Santos, M.M., Venkatesh, B., Tocher, D.R., Castro, L.F. 2016b. Evolutionary functional elaboration of the Elovl2/5 gene family in chordates. Sci Rep., 6:20510.

Morais, S., Castanheira, F., Martinez-Rubio, L., Conceição, L.E.C., Tocher, D.R., 2012. Long chain polyunsaturated fatty acid synthesis in a marine vertebrate: Ontogenetic and nutritional regulation of a fatty acyl desaturase with Δ4 activity. Biochim. Biophys. Acta 1821, 660-671.

Nelson, J.S., 1994. Fishes of the world, 3rd edition ed, New York.

Oboh, A., Betancor, M.B., Tocher, D.R., Monroig, O., 2016. Biosynthesis of long-chain polyunsaturated fatty acids in the African catfish *Clarias gariepinus*: Molecular cloning and functional characterisation of fatty acyl desaturase (fads2) and elongase (elovl2) cDNAs7. Aquaculture 462, 70-79.

Omasits, U., Ahrens, C.H., Müller, S., Wollscheid, B., 2014. Protter: interactive protein feature visualization and integration with experimental proteomic data. Bioinformatics 30, 884-886.

Park, H.G., Park, W.J., Kothapalli, K.S.D., Brenna, J.T., 2015. The fatty acid desaturase 2 (FADS2) gene product catalyzes Δ4 desaturation to yield n-3 docosahexaenoic acid and n-6 docosapentaenoic acid in human cells. The FASEB Journal 29, 3911-3919.

Park, W.J., Kothapalli, K.S.D., Lawrence, P., Tyburczy, C., Brenna, J.T., 2009. An alternate pathway to long-chain polyunsaturates: the FADS2 gene product Δ8-desaturates 20:2n-6 and 20:3n-3. J. Lipid Res. 50, 1195-1202.

490 Pereira, S.L., Leonard, A.E., Mukerji, P., 2003. Recent advances in the study of fatty acid desaturases
491 from animals and lower eukaryotes. Prostaglandins, Leukotrienes and Essential Fatty Acids 68, 97-106.

492 Perica, M.M., Delaš, I., 2011. Essential Fatty Acids and Psychiatric Disorders. Nutr. Clin. Pract. 26,
493 409-425.

494 Psota, T.L., Gebauer, S.K., Kris-Etherton, P., 2006. Dietary Omega-3 Fatty Acid Intake and
495 Cardiovascular Risk. The American Journal of Cardiology 98, 3-18.

496 Ribeiro, R.A., Ozório, R.O.d.A., Batista, S.M.G., Pereira-Filho, M., Ono, E.A., Roubach, R., 2011. Use
497 of Spray-Dried Blood Meal as an Alternative Protein Source in Pirarucu (*Arapaima gigas*) Diets. J.
498 Appl. Aquacult. 23, 238-249.

499 Rivers, J.P.W., Sinclair, A.J., Crawford, M.A., 1975. Inability of the cat to desaturate essential fatty
500 acids. Nature 258, 171-173.

501 Robinson, L., Mazurak, V., 2013. N-3 Polyunsaturated Fatty Acids: Relationship to Inflammation in
502 Healthy Adults and Adults Exhibiting Features of Metabolic Syndrome. Lipids 48, 319-332.

503 Rose, T.M., Henikoff, J.G., Henikoff, S., 2003. CODEHOP (COnsensus-DEgenerate Hybrid
504 Oligonucleotide Primer) PCR primer design. Nucleic Acids Res. 31, 3763-3766.

505 Shanklin, J., Whittle, E., Fox, B.G., 1994. Eight Histidine Residues Are Catalytically Essential in a
506 Membrane-Associated Iron Enzyme, Stearoyl-CoA Desaturase, and Are Conserved in Alkane
507 Hydroxylase and Xylene Monooxygenase. Biochemistry (Mosc). 33, 12787-12794.

508 Tanomman, S., Ketudat-Cairns, M., Jangprai, A., Boonanuntanasarn, S., 2013. Characterization of fatty
509 acid delta-6 desaturase gene in Nile tilapia and heterogenous expression in Saccharomyces cerevisiae.
510 Comp. Biochem. Physiol. B. Biochem. Mol. Biol. 166, 148-156.

511 Tocher, D.R., Leaver, M.J., Hodgson, P.A., 1998. Recent advances in the biochemistry and molecular
512 biology of fatty acyl desaturases. Prog. Lipid Res. 37, 73-117.

513 Tocher, D.R., 2003. Metabolism and Functions of Lipids and Fatty Acids in Teleost Fish. Rev Fish Sci
514 11, 107-184.

515 Tocher, D.R., 2010. Fatty acid requirements in ontogeny of marine and freshwater fish. Aquacult. Res.
516 41, 717-732.

517 Torres, F.G., Malásquez, M., Troncoso, O.P., 2015. Impact and fracture analysis of fish scales from
518 Arapaima gigas. Materials Science and Engineering: C 51, 153-157.

519 Tsirigos, K.D., Peters, C., Shu, N., Käll, L., Elofsson, A., 2015. The TOPCONS web server for
520 consensus prediction of membrane protein topology and signal peptides. Nucleic Acids Res. 43, W401-
521 W407.

522 Turchini, G.M., Torstensen, B.E., Ng, W.-K., 2009. Fish oil replacement in finfish nutrition. Reviews
523 in Aquaculture 1, 10-57.

524 Veríssimo, J., 1895. A pesca na Amazônia. Livraria classica de Alves.

525 Wall, R., Ross, R.P., Fitzgerald, G.F., Stanton, C., 2010. Fatty acids from fish: the anti-inflammatory
526 potential of long-chain omega-3 fatty acids. Nutr. Rev. 68, 280-289.

527 Wang, S., Monroig, Ó., Tang, G., Zhang, L., You, C., Tocher, D.R., Li, Y., 2014. Investigating long-
528 chain polyunsaturated fatty acid biosynthesis in teleost fish: Functional characterization of fatty acyl
529 desaturase (Fads2) and Elovl5 elongase in the catadromous species, Japanese eel Anguilla japonica.
530 Aquaculture 434, 57-65.

531 Xie, D., Chen, F., Lin, S., Wang, S., You, C., Monroig, Ó., Tocher, D.R., Li, Y., 2014. Cloning,
532 Functional Characterization and Nutritional Regulation of Δ6 Fatty Acyl Desaturase in the Herbivorous
533 Euryhaline Teleost Scatophagus Argus. PLoS ONE 9, e90200.

534 Zheng, X., Seiliez, I., Hastings, N., Tocher, D.R., Panserat, S., Dickson, C.A., Bergot, P., Teale, A.J.,
535 2004. Characterization and comparison of fatty acyl Δ6 desaturase cDNAs from freshwater and marine
536 teleost fish species. Comp. Biochem. Physiol. Biochem. Mol. Biol. 139, 269-279.

537 Zheng, X., Tocher, D.R., Dickson, C.A., Bell, J.G., Teale, A.J., 2005. Highly unsaturated fatty acid
538 synthesis in vertebrates: new insights with the cloning and characterization of a delta6 desaturase of
539 Atlantic salmon. Lipids 40, 13-24.

540 Zheng, X., Ding, Z., Xu, Y., Monroig, O., Morais, S., Tocher, D.R., 2009. Physiological roles of fatty
541 acyl desaturases and elongases in marine fish: Characterisation of cDNAs of fatty acyl Δ6 desaturase
542 and elovl5 elongase of cobia (*Rachycentron canadum*). Aquaculture 290, 122-131.

543

544

545

546 **Tables**

547 **Table 2.** Accession number of sequences used phylogenetic analysis.

	Accession number	
Species	**FADS2**	**FADS1**
HSA- *Homo Sapiens*	NP_004256.1	NP_037534.3
MDO- *Monodelphis domestica*	-	H9H609
ASI- *Alligator sinensis*	XP_006033391.1	XP_006033402.1
GGA- *Gallus gallus*	NP_001153900.1	XP_421052.4
LCH- *Latimeria chalumnae*	XP_005988034.1	XP_005988035.1
CMI - *Callorhinchus milii*	XP_007885636.1	XP_007885635.1
SCA- *Scyliorhinus canicula*	AEY94455.1	-
DRE- *Danio rerio*	NP_571720.2	-
SSA- *Salmo salar*	NP_001117047.1	-
ONI-*Oreochromis niloticus* (a)	XP_005470661.1	-
ONI-*Oreochromis niloticus* (b)	XP_003440520.1	-
TMA - *Thunnus maccoyii*	ADG62353.1	-
GMO - *Gadus morhua*	AAY46796	-
BFL - *Branchiostoma floridae*	XP_002586930.1	

548

549

550

551

552

553 **Table 1.** Primer sets and corresponding PCR conditions.

Primer set function	Primer name	Primer sequence	Initial denaturation	Cycles	Denaturation	TM	Extension (size bp)	Final extension
Degenerate primers	FADS2degen_F	GCGCCTCCGCCAAytggtggaayc	98ºC /10s	40	98ºC /1s	54ºC/5s	72ºC/10s	72ºC/1min
	FADS2degen_R	TGGCCGGAGAACcartcrttraa						
Gene specific Race primers	3RC_AgigasFADS_F	ACCTAAAGGGTGCTTCAGCCAACT	98ºC /10s	20	98ºC /1s	62ºC/5s	72ºC/15s	72ºC/1min
	5RC_AgigasFADS_R	GTTCGGAACAAGCCCTCTTTCTC						
Nested Gene specific Race Primers	N3RC_AgigasFADS_F	GTTTCTGGAGAGCCACTGGTTTGT	98ºC /10s	35	98ºC /1s	62ºc/5s	72ºC/8s	72ºC/1min
	N5RC_AgigasFADS_R	CTGCGTTTTTCTGGCGGTCTAAG						
Full ORF	AgigasFADS_ORF_F	ATATTGCCAGAGGATGGATG	98ºC /10s	20	98ºC /1s	56ºC/5s	72ºC/22s	72ºC/1min
	AgigasFADS_ORF_R	GGGCCTCATTACATTCAATAAA						
Restriction site primers for cloning	AgigasFADS_pYES_KpnI_F	CCCGGTACCAAGATGGGCGGCGGGGGGCA	98ºC /10s	35	98ºC /1s	67ºC/5s	72ºC/20s	72ºC/1min
	AgigasFADS_pYES_XbaI_R	CCCTCTAGAGGGGTTACTTGTGGAGATACGCATC						

555 **Table 3:** Functional characterization of the *Arapaima gigas* Fads2 in yeast. Conversions were
556 calculated according to the formula (product area / (product area + substrate area)) ×100.

FA substrate	FA product	% conversion
18:3n-3	18:4n-3	25.8
18:2n-6	18:3n-6	16.1
20:3n-3	20:4n-3	5.8
20:2n-6	20:3n-6	3.8
20:4n-3	20:5n-3	nd
20:3n-6	20:4n-6	nd
22:5n-3	22:6n-3	nd
22:4n-6	22:5n-6	nd

557 nd, not detected

558

559

Figures and legends

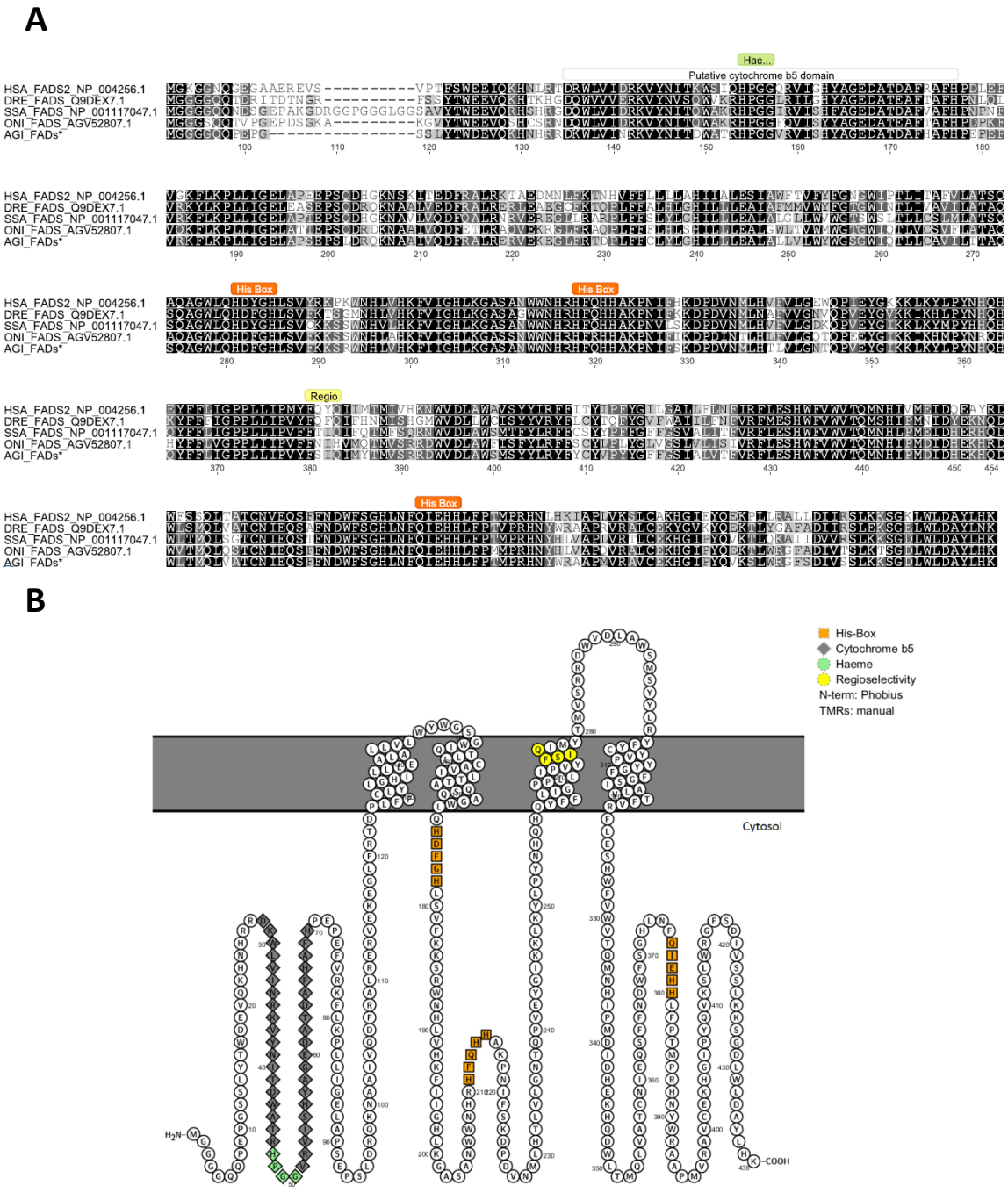

Figure 1. Sequence analysis of *Arapaima gigas* Fads2. **A,** FADS sequence alignment, white: Cytochrome b5-like domain, green: heme binding motif, orange: conserved histidine boxes, and yellow reported regioselectivity residues. **B,** Predicted 2D topology of *Arapaima gigas* Fads color code is maintained.

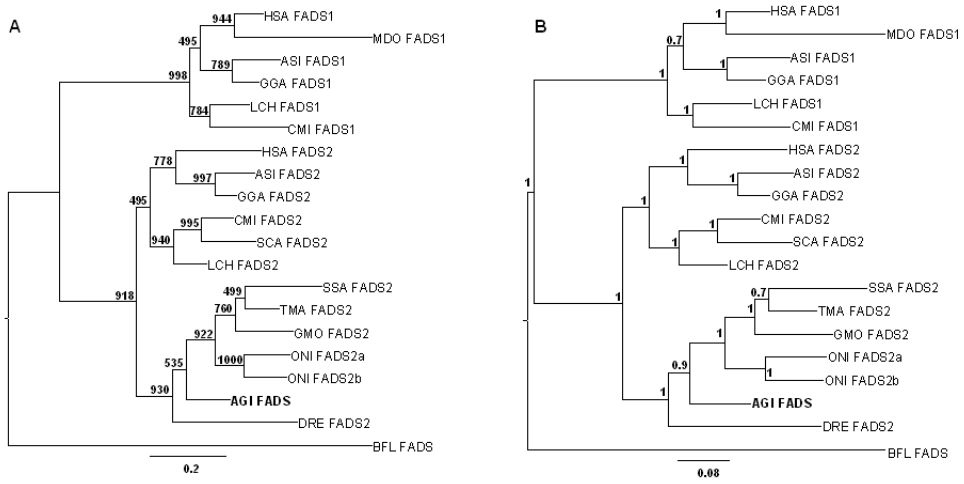

Figure 2: Molecular phylogenetic analysis. A - Maximum likelihood phylogenetic analysis, node values indicate bootstrap replicates; **B –** Bayesian phylogenetic analysis node values indicate posterior probabilities. HSA- *Homo sapiens,* MDO - *Monodelphis domestica,* GGA - *Gallus gallus,* ASI - *Alligator sinensis,* LCH - *Latimeria chalumnae* DRE- *Danio rerio*; AGI- *Arapaima gigas*; ONI - *Oreochromis niloticus*; SSA- *Salmo salar*; GMO - *Gadus morhua*; TMA- *Thunnus maccoyii*; CMI - *Callorhinchus milii,* SCA- *Scyliorhinus canícula*. BFL – *B. floridae*.

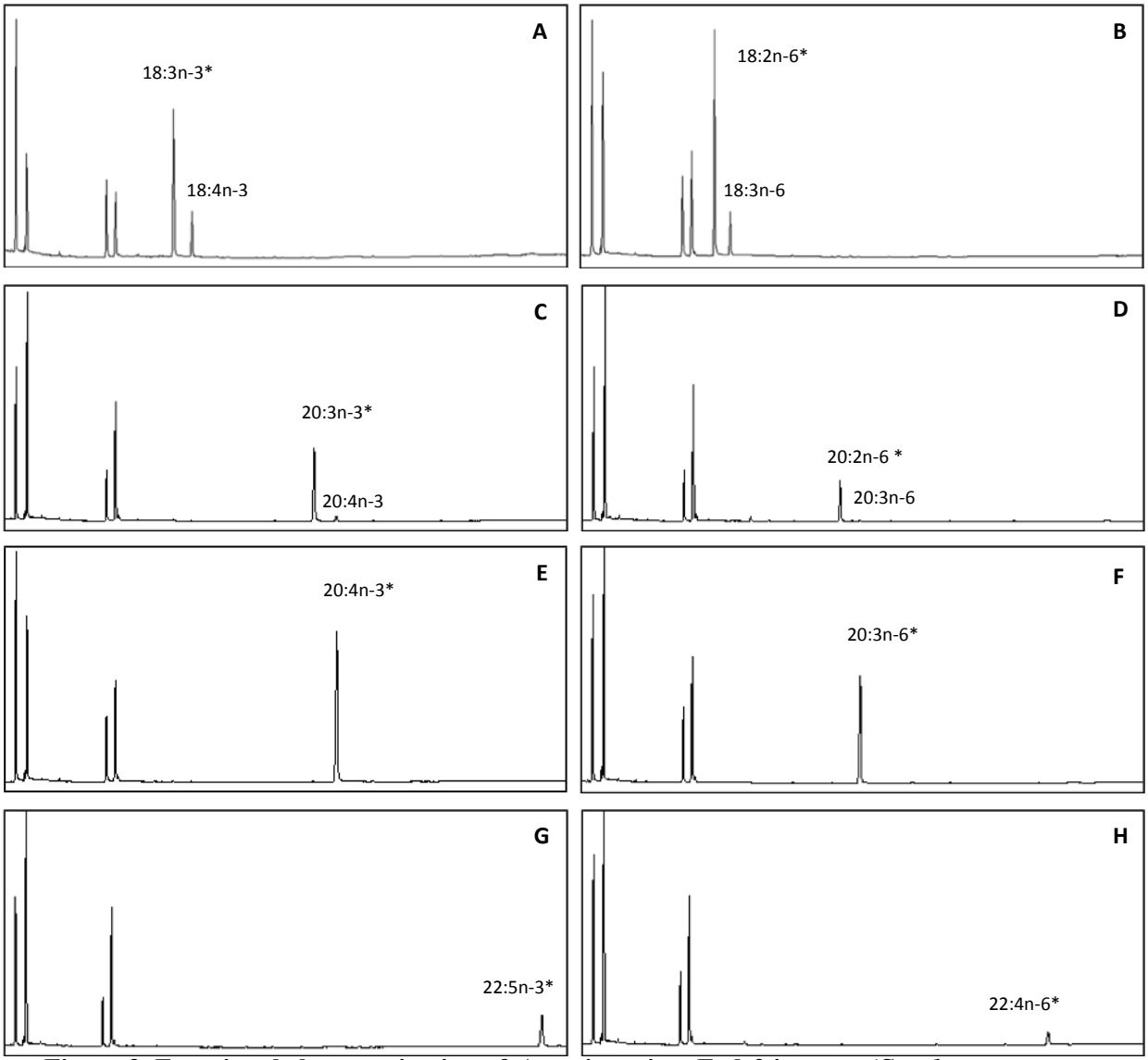

Figure 3. Functional characterization of *Arapaima gigas* Fads2 in yeast (*Saccharomyces cerevisiae*). Fatty acid (FA) profiles were determined after the yeast were grown in the presence of exogenously added substrates indicates in each case by (*). Peaks 1-4 in all panels correspond to yeast endogenous FA, namely **1 -** (16:0), **2 -** (16:1n-7), **3 –** (18:0) and **4 –** (18:1n-9). FA derived from the exogenously added substrates or elongation products are indicated accordingly in each panel above the corresponding product.

Supplementary material 1

2D topology prediction results

601

Method	TM- helix position starting from 1			
TOPCONS	TM1: 124-145,	TM2: 151-172,	TM3: 258-279,	TM4: 300-321
OCTOPUS	TM1: 124-145,	TM2: 146-167,	TM3: 257-278,	TM4: 290-321
Philius	TM1: 126-147,	TM2: 152-173,	TM3: 259-281,	TM4: 300-324
PolyPhobius	TM1: 125-148,	TM2: 152-172,	TM3: 259-282,	TM4: 296-321
SCAMPI	TM1: 123-144,	TM2: 152-173,	TM3: 258-279,	TM4: 300-321
SPOCTOPUS	TM1: 124-145,	TM2: 146-167,	TM3: 257-278,	TM4: 290-321

602

603

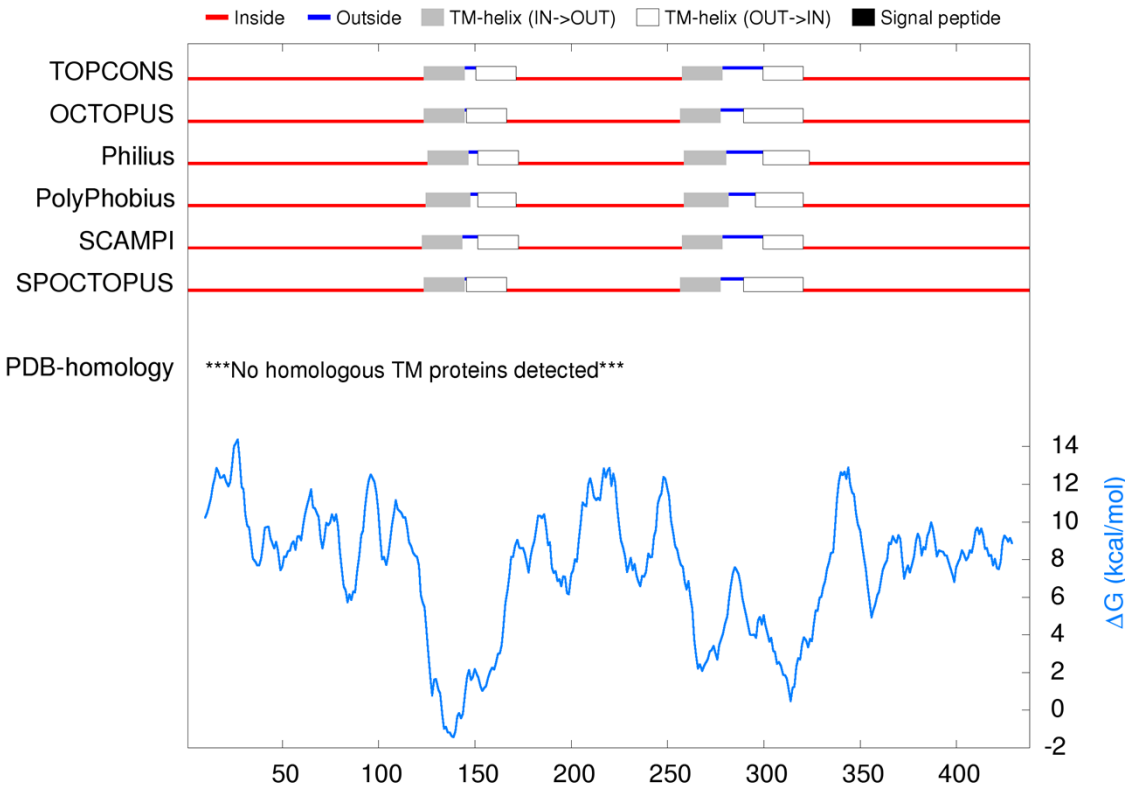

604

605